

Control of an XY Nano-Positioning Table for a Compact Nano-Machine Tool*

Guilherme Jorge MAEDA**, Kaiji SATO**, Hitoshi HASHIZUME*** and Tadahiko SHINSHI***

This paper describes the control of an XY nano-positioning table for a compact nano-machine tool. The aim of its controller design is to provide (1) high motion accuracy, (2) high robustness to disturbance forces and (3) high bandwidth. The controller has a PID element as a tandem compensator and a feedforward compensator. A bandpass filter is added so that the table system can show the mentioned specifications (1) and (2). The reference following characteristic and the robustness to disturbance forces are examined and evaluated theoretically and experimentally. The results prove that the table control system is suitable for a compact ultraprecision machine tool, attaining high positioning accuracy and frequency response up to 500 Hz in a circular motion of a 100 nm radius.

Key Words: Nano-Positioning, Precision Machine Tool, PID Control, Bandpass Filter, 2 DOF Control, Digital Control, Planar Motor, VCM

1. Introduction

Improvement of machinery for manufacturing microstructures must keep pace with the increasing use of microdevices and miniaturization of products. MEMs manufacturing processes is one of the methods used for fabrication of micromechanical structures, basically by extending methods used in the production of integrated circuits. However, due to its non-mechanical nature, processes available for MEMs manufacture restrain the creativity of design usually leading to simple-shaped⁽¹⁾ and silicon-made parts. Production of arbitrary-shaped microstructure parts using different materials, including metallic ones, can be achieved through ultraprecision machining. However, conventional ultraprecision machine tools have some drawbacks: complicated design, big size, and high-energy consumption lead to an expensive output and waste of resources.

At present, research efforts have been conducted in order to overcome the above mentioned problems through the design of more efficient and smaller ultraprecision ma-

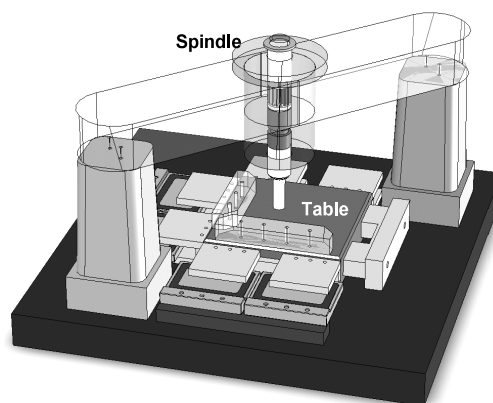


Fig. 1 Schematic view of the compact nano-machine tool

chine tools, so that a drastic reduction in the cost of production of micro-machined parts is expected⁽²⁾. Economical reasons are not the only motivation for smaller machine tools. Technically, as described by Kussul et al. (2002), the reduced inertia of such machines decreases vibration and facilitates the control for precision positioning.

The authors have been studying a compact nano-machine tool that is small and capable of machining 3D microstructures with nanometric precision. Figure 1 shows the concept of the compact nano-machine tool in this research. In this machine, the workpiece is positioned by an XY table⁽⁴⁾ and the cutting tool — a precision aerostatic spindle^{(5), (6)} — is positioned in the Z direction.

* Received 28th October, 2005 (No. 05-4228)

** Interdisciplinary Graduate School of Science and Engineering, Tokyo Institute of Technology, 4259-G2-17 Nagatsuta, Midori-ku, Yokohama 226-8502, Japan.
E-mail: m05maeda@pms.titech.ac.jp

*** Precision and Intelligence Laboratory, Tokyo Institute of Technology, 4259 Nagatsuta, Midori-ku, Yokohama 226-8503, Japan

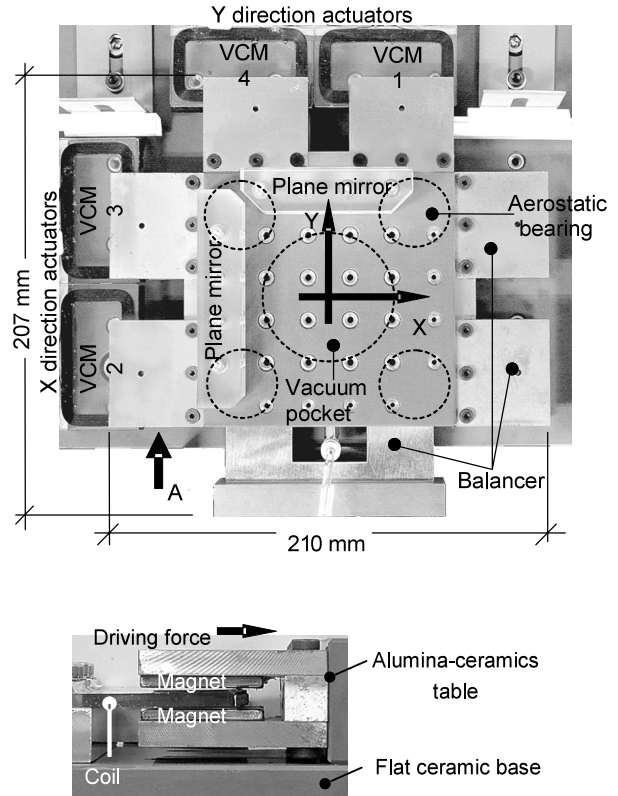
A limiting factor in ultraprecision machining is the positioning characteristic of the machine tool. The attainable machining quality depends on the ability of the positioning system to travel along a desired contour and position the workpiece with appropriate accuracy. Conventional design concepts used in precision positioning systems with multiple degrees of freedom are: a) parallel mechanisms and b) stacked 1DOF (degree of freedom) motion axes. The concept a) leads to kinematic redundancies and singularities, being costly in terms of design and control. The concept b), based on the superposition of single-degree-of-freedom systems, propagates errors on the subsequent directions. Although the two concepts are often used for precision positioning, neither of them are suitable for miniaturization, because their mechanical design is intrinsically complex, involving many parts and linkages. On the other hand, single-moving-part with multiple-degree-of-freedom systems have been researched due to its mechanical simplicity and feasibility for compactness. Still, coupling among movement of axes are observed in most of these researches and methods to circumvent this problem is always left in charge of the controller: decoupling the movement by compensating the control signals as did Tomita (1998), or by considering the coupling interference among axes as external disturbances^{(8),(9)}. The mechanical design of the XY table in this paper was researched in Shinno et al. (2004), where also a preliminary controller version was designed. The system has multiple degrees of freedom, and, because the table is driven at its center of mass, the problem of coupling among axes movement was mechanically solved.

With a suitable mechanical system for nano-positioning available, the controller is entrusted to assure the desired performance. Since the table is direct driven, rejection of external sources of vibration and disturbance forces caused during cutting are totally in charge of the control servo-stiffness, given that no mechanical stiffness provided by gear reductions or lead screws are present.

This paper is focused on the controller design of the XY table of the compact nano-machine. This paper is organized in 5 sections. Section 2 concerns the mechanical design of the table. Section 3 explains the control system, a 2DOF controller consisting of a PID compensator, a feedforward compensator and a bandpass filter. Section 4 shows the positioning performance results and section 5 proposes planned trajectories in order to achieve better results.

2. Mechanical Design

In order to attain nano-positioning resolution, aerostatic bearings and voice coil motors (VMCs) allow a table motion free from friction and thermal deformation. The table is symmetrically designed with respect to the X and Y axes, therefore, the dynamic characteristic for both axes



View A: Detail of the coil and magnets.
 Fig. 2 Structural configuration of the table

Table 1 Mechanical specification

Mass of the table	4.1 kg
Material of the table	Alumina-ceramics
Maximum stroke (X, Y)	18 mm
Maximum driving force	9.4 N
Z direction bearing stiffness	84.3 N/μm
Sensor linear resolution	1.24 nm
Sensor angular resolution	0.1 μrad

are identical, as well as the controllers.

The structure of the controller can be simplified because the combination of the forces applied by each actuator drives the table at its center of mass, eliminating interdependencies between axes⁽⁴⁾. This configuration relieves the controller from decoupling compensators, synchronizer motion algorithms or any other contrived method.

Each axis, X and Y, is driven by two VCMs, that is, VCM 2 and 3, and 1 and 4, respectively (Fig. 2) and each VCM is powered by its own current amplifier. All the VCMs are used for driving the table in the θ direction. The table has a travel range to machine workpieces up 10 mm × 10 mm on the XY plane. The maximum driving force provided by the VCMs is 9.4 N per axis at 7 A per channel. The table position is measured with a laser interferometer with 1.24 nm of resolution in the X and Y direction and 0.1 μrad in the θ direction.

High stiffness is helpful to increase the resistance to forces introduced by the cutting tool, ensuring low vibration during machining. Bearing stiffness in the Z direction is increased preloading the aerostatic bearing. Shinno et al. (2004) shows that the stiffness of the aerostatic bearing increases more than tenfold (from 7.3 N/ μm to 84.3 N/ μm) when using a vacuum pump that draws air from the vacuum pocket, shaped on the bottom part of the table.

3. Control System

The mechanism has a simple structure. As a controller for the mechanism, a simple 2DOF controller, is selected. The controller is easy to design and adjust.

3.1 Controller structure

Figure 3 shows the distribution of the control signals among the four VCMs; where M_t is the mass of the table, J the rotational inertia of the table and L the distance between the driving axis and the center of mass. The control signal for each direction is divided between two actuators (X direction: actuators 2 and 3, Y direction: actuators 1 and 4) while the rotational control signal is divided equally among the four actuators. The reference for the θ direction is always zero given that the table is supposed not to have rotational motion.

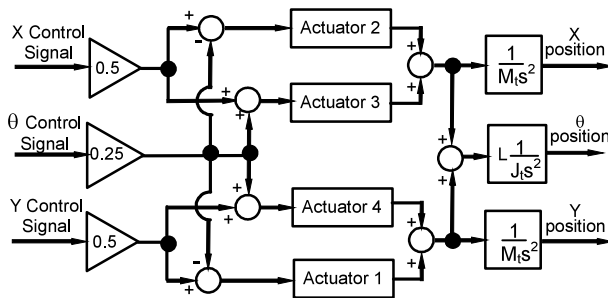


Fig. 3 Control signal distribution among the VCMs

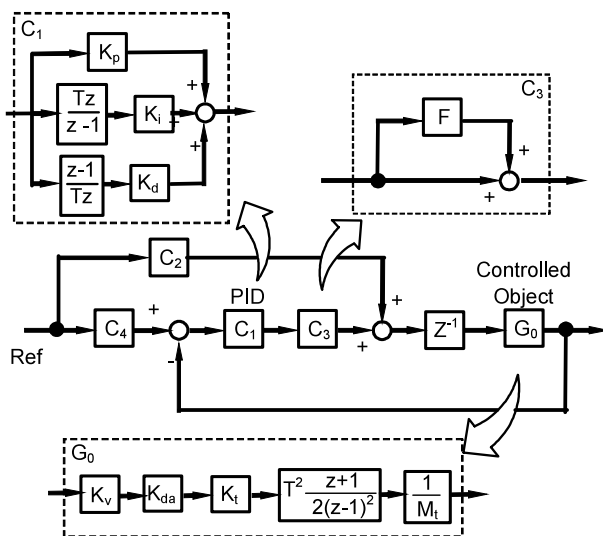


Fig. 4 Control structure of the X and Y direction

Figure 4 shows the structure of the controller with respect to the X and Y directions. The 2DOF controller is composed of a PID compensator (C_1), a feedforward loop (C_2 and C_4) and a bandpass filter (F). In the θ direction the controller does not have a feedforward loop since the reference input is always zero and no severe reference tracking is demanded, supporting efforts to design a simple controller.

The parameters in Fig. 4 are described as follow:

K_p : PID proportional gain

K_i : PID integral gain

K_d : PID derivative gain

K_t : Thrust constant

K_v : Amplifier gain

K_{da} : DA converter gain

F : bandpass filter

T : Sampling time

3.2 Design procedure

The 2DOF controller is designed through a procedure that can be divided in two steps:

- 1) PID gain adjustment for lower disturbance gain

Disturbance gain (displacement/disturbance) is influenced by the PID gains and the bandpass filter F shown in Fig. 4. Larger PID gains decrease the disturbance gain and improve the disturbance rejection characteristic of the system. Higher derivative gain is useful for reducing a resonant gain peak. However, it often deteriorates the positioning accuracy of the system and increases residual vibration. The bandpass filter is adjusted so as to eliminate the gain peak and keep high positioning accuracy with a lower derivative gain. More details with experimental results are found in sub-section 4.1.

- 2) Determination of C_2 and C_4 for wide frequency range at which the gain keeps flat

In order to increase the bandwidth and achieve small trajectory following errors in X and Y directions, a feedforward compensator was implemented.

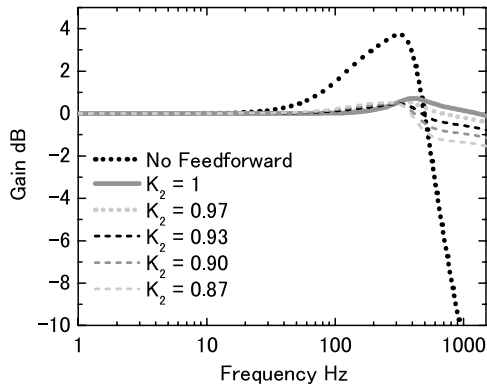
Since the movement of the table is friction-free, the dynamic model does not include non-linear effects, being, at least in low frequencies, free from uncertainties. The inverted model is then, a suitable candidate as a feedforward compensator⁽¹⁰⁾.

The ideal transfer function of the feedforward compensator is given by the inverse of the product $z^{-1}G_0(z)$, where $G_0(z)$ is:

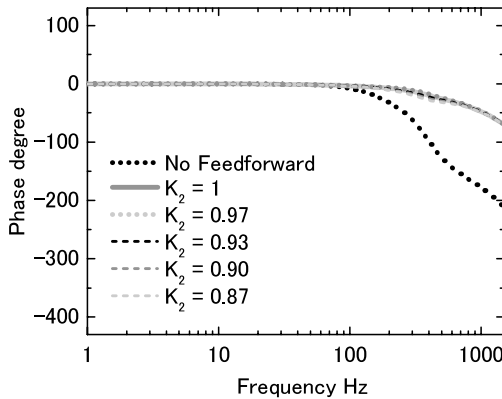
$$G_0(z) = \frac{K_v K_t K_{da}}{M_t} \cdot \frac{(Tz)^2}{(z-1)^2} \cdot \frac{z+1}{2z^2} \quad (1)$$

where T is the controller sampling time.

The inverse of $z^{-1}G_0(z)$ leads to a transfer function with the numerator having higher order than the denominator, thus, being impossible to implement. As an alternative, the implementable transfer functions C_2 and C_4 can be set as:



(a)



(b)

Fig. 5 Simulated reference following characteristic in the frequency domain

$$C_2(z) = K_2 C_4 z G_0(z)^{-1} = K_2 \frac{M_t}{K_v K_t K_{da}} \cdot \frac{(z-1)^2}{(Tz)^2} \quad (2)$$

$$C_4(z) = \frac{z+1}{2z^3} \quad (3)$$

where C_2 becomes the implementable feedforward transfer function (including a correction factor K_2) and C_4 a delay.

Figure 5 shows the reference following characteristics in the frequency domain. By setting $K_2 = 1$ the gain of the frequency response in Fig. 5 (a) becomes almost flat, but not perfectly (continuous line). This imperfection, given as a resonant peak around 250 Hz, has a small amplitude of less than 1 dB but it is not negligible for ultraprecision position motion control. In order to reduce the negative influence on the motion accuracy, K_2 is adjusted. Adjustment of K_2 is also useful when the system parameters change or are uncertain. Experimental results of this adjustments are shown in sub-section 4.2.

4. Control Performance

4.1 Disturbance rejection characteristics

The PID parameters were tuned to reduce disturbances caused by external sources and vibrations in steady state, while attaining high performance tracking of reference. Figure 6 shows the effect of increasing the deriva-

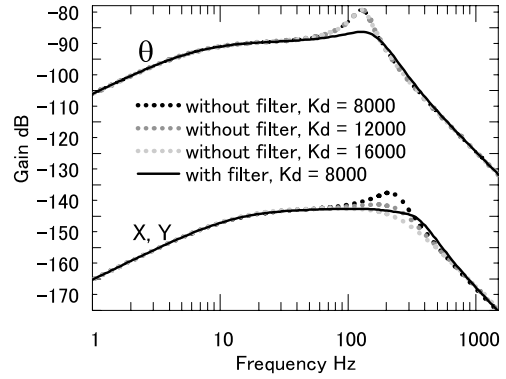
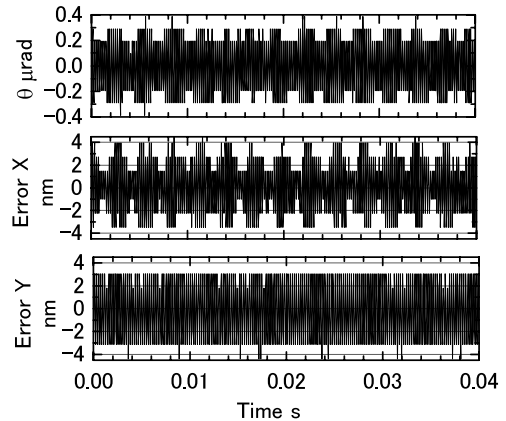
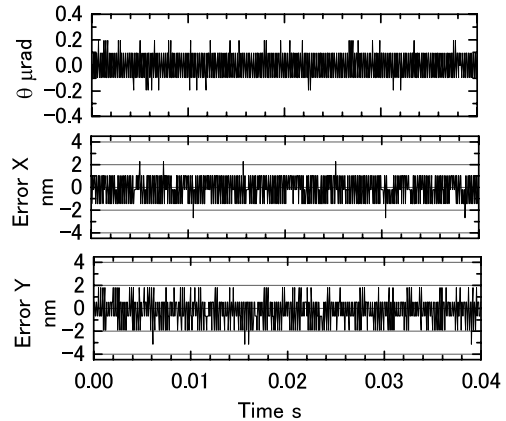


Fig. 6 Disturbance gain characteristics



(a) $K_d = 16000$



(b) $K_d = 8000 + \text{bandpass filter}$

Fig. 7 Effects of the bandpass filter and the derivative gain on steady state

tive gain for the X and Y direction controllers, while the derivative gain in the θ direction controller was not changed. As mentioned in sub-section 3.2, a higher derivative gain value (K_d) reduces the resonant peak and improves the disturbance rejection characteristic. However, the increase in the derivative gain increases vibrations in steady state (Fig. 7 (a)), including the θ direction (although its derivative gain was not changed), limiting motion accuracy. In order to respect both desired characteristics — disturbance rejection and low vibration — a

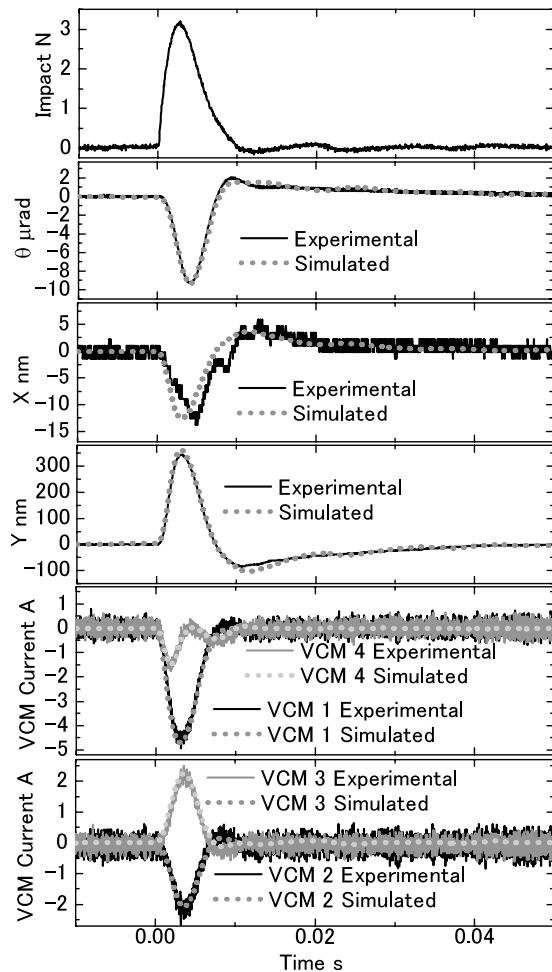


Fig. 8 Disturbance impact test

bandpass filter F is added after the control signal of the X , Y and θ directions, as shown in Fig. 4.

With the inclusion of the bandpass filter, the peaks on the disturbance gain characteristic curves (solid line in Fig. 6) were significantly reduced in all directions allowing the use of smaller derivative gains.

The decrease of the derivative gain and the use of the bandpass filter reduced the steady state vibration amplitude to values close to the sensor resolution as seen in Fig. 7 (b).

The disturbance rejection characteristic is evaluated experimentally with an impact test. Figure 8 shows the robustness performance to an impact disturbance. Using an impact hammer previously calibrated, an impact force was applied approximately 45 mm parallel with the Y axis of symmetry in order to produce disturbances in Y and θ directions. Because it is impossible to create an impact perfectly normal to the X direction, a small displacement in the X direction occurred. According to the analysis using the dynamic model, 3.5% of the total impact force was transmitted to the X direction. The table recovers its position within 0.05 s after an impact of 3.2 N. This result shows that the system has high robustness.

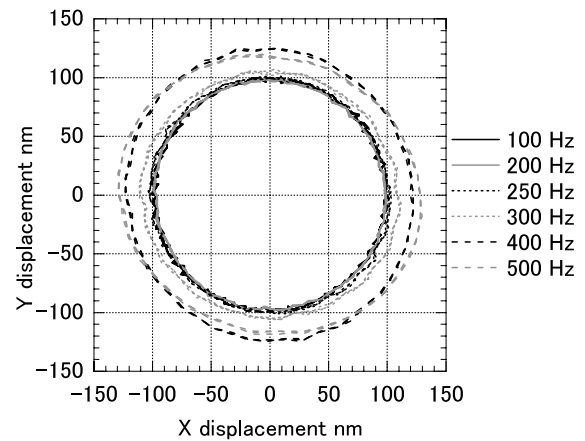
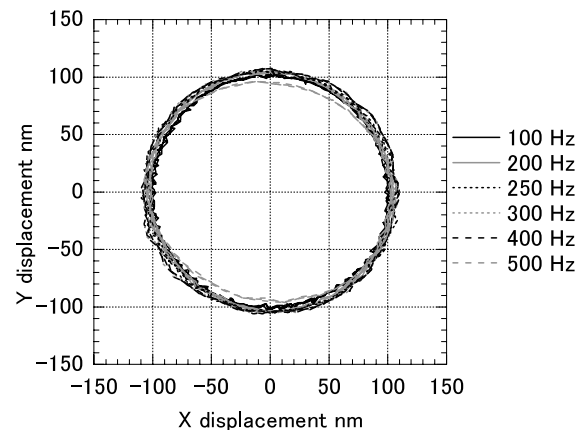
(a) $K_2 = 1$. Standard feedforward gain(b) $K_2 = 0.87$. Experimentally adjusted feedforward gain

Fig. 9 100 nm radius circular motion

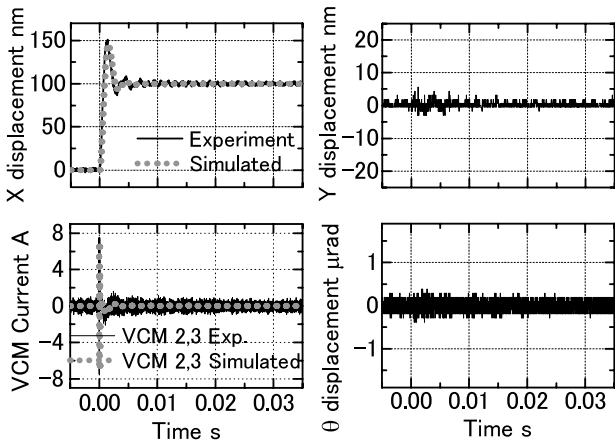
4.2 Trajectory following characteristics

Figure 9 (a) shows the trajectory following performance for a circular motion of 100 nm radius at several frequencies with $K_2 = 1$. The tracking error is small until 250 Hz (4 nm), but it increases at higher frequencies attaining 25 nm at 400 Hz. Such behavior was expected as the simulated Bode diagram in Fig. 5 shows the resonant peak affecting this range of frequency.

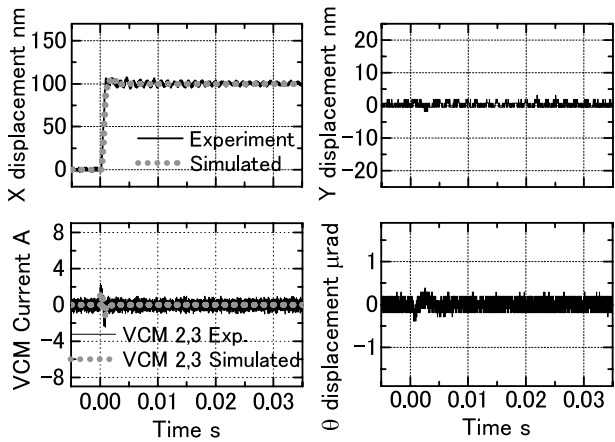
Aiming better trajectory tracking performance above 250 Hz, the K_2 value was experimentally fine-tuned through frequency response tests. From these adjustments, using $K_2 = 0.87$, smaller maximum tracking errors of 7 nm were obtained for motions up to 500 Hz (Fig. 9 (b)).

5. Improvement of Tracking Performance

A 100 nm step response applied only in the X direction and its influences in Y and θ displacements are shown in Fig. 10 (a). Negligible fluctuations in Y and θ displacements prove the system has, intrinsically, independent axis motion, given that no decoupling method needed to be used. Also from the same figure, it is possible to verify the agreement between the experimental results and the simulated results with the non-linear model, which includes the



(a) Conventional step input response



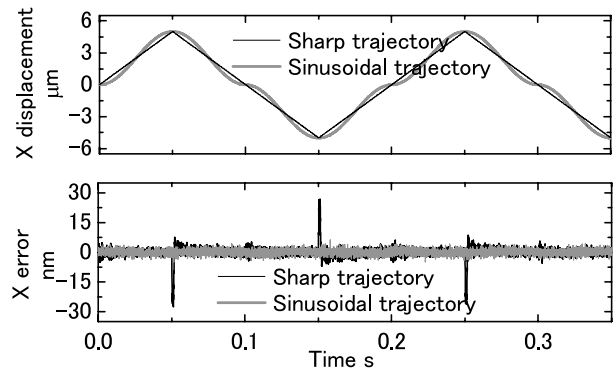
(b) Sinusoidal step input response

Fig. 10 Step response in the X direction and its influences in the Y and θ directions

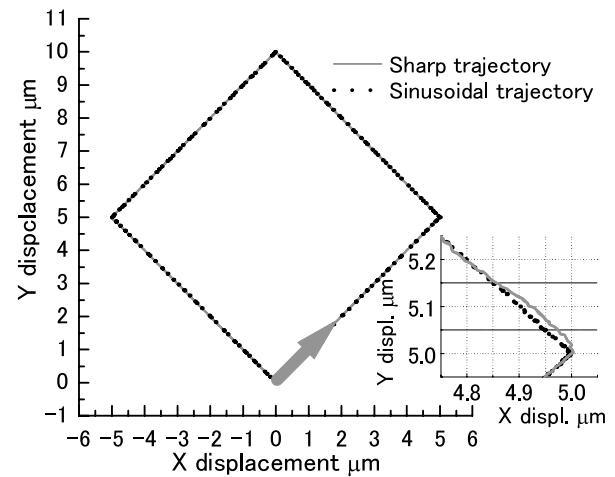
saturation effect of the amplifiers.

In order to improve the transient step responses, which means to reduce overshoot and settling time, an alternative step-like input is used. Figure 10(a) shows that the current in the two VCMs of X direction saturates at 7 A, leading to overshoot and slowing the settling time. Respecting the fact that “the trajectory should be such that the force is allowable and can be generated by the actuating device” (Lambrechts et al., 2004, p.4637), a reference that does not saturate the actuators will result in better response. Thus, based on the fact that the system has small tracking error in a 500 Hz circular motion (Fig.9(b)), a step-like input reference constructed from a quarter of a 500 Hz sine wave was used as the new shaped reference. Figure 10(b) shows the response of the system when using the new reference. As expected, the table follows accurately the sinusoid reference so that the overshoot and the settling time could be remarkably improved without saturation of the actuators.

Square tracking motion was evaluated using a conventional sharp trajectory. The motion consists of a square $10\mu\text{m}$ diagonally lengthened and 0.2 seconds of period.



(a) X axis square motion



(b) Square motion trajectory

Fig. 11 Square motion in the micrometer range

As saturation occurs again, large errors at the corners of the square are observed. The same principle of shaped reference used in the step input case is applied once more. Tracking motions in the X direction of the conventional sharp trajectory and the “smooth” sinusoidal trajectory are shown in Fig. 11 (a). The motion in the Y direction is not shown as it has basically the same behavior as in the X direction. As shown in Fig. 11, the sharp trajectory tracking response shows a maximum error of 30 nm occurring at the corners. The sinusoidal reference leads to a maximum error of 5 nm.

6. Conclusions

A suitable and simple controller for the XY nano-positioning table was designed. Its design procedure was discussed and experiments were done in order to evaluate the performance.

The use of a bandpass filter is effective to improve the disturbance rejection characteristics and motion accuracy, resulting in a steady-state vibration amplitude close to the sensor resolution. High frequency motion with small tracking error were attained with the adjustment of the feedforward compensator. Planning the trajectory so that saturation of actuators is avoided shows to be an ef-

fective way to decrease overshoot and reference tracking error in point-to-point and continuous motion. As a result, the proposed control provides nanometric motion accuracy, robustness, and high bandwidth; three fundamental characteristics in a machine tool positioning system.

As a next step, the controlled XY nano-positioning table and the aerostatic spindle will be assembled as a single system, concluding the compact nano-machine tool.

References

- (1) Hatamura, Y., Nakao, M. and Sato, T., Construction of an Integrated Manufacturing System for 3D Microstructure—Concept, Design and Realization, *Ann. CIRP*, Vol.46, No.1 (1997), pp.313–318.
- (2) Kussul, E., Rachkovskij, D., Baidyk, T. and Talayev S., *Micromechanical Engineering: A Basis for the Low-Cost Manufacturing of Mechanical Microdevices Using Microequipment*, *J. Micromech. Microeng.*, Vol.6, No.4 (1996), pp.410–425.
- (3) Kussul, E., Baidyk, T., Ruiz, L., Caballero, A. and Velasco, G., Development of Low-Cost Microequipment, *Proc. Int. Simp. on Micromechatronics and Humans Science*, Nagoya, Japan, (2002), pp.125–134.
- (4) Shinno, H., Hashizume, H., Yoshioka, H., Komatsu, K., Shinshi, T. and Sato, K., X-Y- θ Nano-Positioning Table System for a Mother Machine, *Ann. CIRP*, Vol.53, No.1 (2004), pp.337–340.
- (5) Shinshi, T., Hayashi, T., Hashizume, H., Sato, K. and Shimokohbe, A., A Precision Aerostatic Spindle Incorporating an Axial Positioning Function for a Compact Nano-Machine Tool, *Proc. 1st Int. Conf. on Positioning Technology*, Hamamatsu, Japan, (2004), pp.449–450.
- (6) Shinshi, T., Inami, Y., Hashizume, H., Sato, K. and Shimokohbe, A., An Active Aerostatic Spindle with an Axial-Positioning Actuator for Machining Ultra-Micro Scale Structures, *Proc. LEM21*, Nagoya, Japan, (2005), pp.1015–1018.
- (7) Tomita, Y. and Koyanagawa, Y., Study on a Surface Motor Driven Precise Positioning System, *J. Dyn. Syst., Meas. Contr.*, Vol.3, No.2 (1998), pp.113–119.
- (8) Dejima, S., Gao, W., Katakura, K., Kiyono, S. and Tomita, Y., Dynamic Modeling, Controller Design and Experimental Validation of a Planar Motion Stage for Precision Positioning, *Precision Eng.*, Vol.29, No.3 (2005), pp.289–298.
- (9) Gu, J., Kim, W.-J. and Verma, S., Nanoscale Motion Control with a Compact Minimum-Actuator Magnetic Levitator, *ASME J. Dyn. Syst., Meas. Contr.*, Vol.127, No.3 (2005), pp.433–442.
- (10) Devasia, S., Robust Inversion-Based Feedforward Controllers for Output Tracking under Plant Uncertainty, *Proc. American Control Conf.*, Chicago, U.S.A., (2000), pp.497–502.
- (11) Lambrechts, P., Boerlage, M. and Steinbuch, M., Trajectory Planning and Feedforward Design for High Performance Motion Systems, *Proc. American Control Conf.*, Boston, U.S.A., (2004), pp.4637–4642.